To appear: *Proceedings Coastal Sediments '03*, May 2003.

NUMERICAL SIMULATION OF SEDIMENT PATHWAYS AT AN IDEALIZED INLET AND EBB SHOAL

Adele Militello[1] and Nicholas C. Kraus[2]

Abstract: Bypassing at inlets can occur across the ebb shoal, through tidal exchange, and by episodic collapse of shoals. To examine ebb-shoal and tidal exchange bypassing in a systematic way, we investigated sediment pathways at an idealized inlet with a coupled tide, wave, and sediment transport-morphology change numerical modeling system. The idealized inlet, ebb shoal, and channel were devised to test the coupled modeling system and isolate sediment transport pathways driven by wave and tidal forcing. The inlet, channel, ebb shoal, and bay dimensions approximate those of Shinnecock Inlet, New York. Five simulations consisting of tide forcing, wave forcing (fair-weather and storm), and combined tide and wave forcing were conducted. Patterns of calculated morphology change followed those found in nature. Simulations with waves impounded sand against the updrift jetty and eroded the bottom in the nearshore area on the downdrift side of the inlet. Wave breaking on the ebb shoal primarily moved material updrift, but also flattened the shoal by eroding the top and depositing material around its perimeter. For the forcing conditions examined, waves were the dominant transport mechanism. Tidal currents modified the morphology change primarily at the inlet entrance and on the updrift side of the ebb shoal by opposing the current during the flood tide.

INTRODUCTION

Morphology change at tidal inlets is controlled by the net bypassing rate, tidal transport through the inlet, and variations in features (bathymetry, structures, etc.) where localized scour and shoaling take place. Common morphologic responses to wave and tide forcing are: bypassing at the ebb shoal, skewing of the ebb shoal, migration of the inlet channel thalweg, development of tip shoals, impoundment at the updrift jetty, beach erosion near the downdrift jetty, and scour holes inside the inlet adjacent to the jetty tips. Shinnecock Inlet, Long Island, New York is an example where all of these responses have been observed. The semi-circular ebb-tidal shoal is skewed to the west owing to the transport driven by waves primarily from the southeast (Militello et al. 2001). Militello and Kraus (2001a, b) found that advection of the inlet ebb jet by the ocean tide contributes to realignment of the channel thalweg at Shinnecock Inlet.

Bruun and Gerritsen (1959) studied bypassing modes at tidal inlets and introduced the concepts of (1) bypassing on the "offshore bar" or ebb shoal, and (2) bypassing through tidal exchange. Episodic bypassing is a third mode (Gaudiano and Kana 2000), not discussed here. Recently, an aggregate model of sediment bypassing and volume change of inlet features was developed that is based on knowledge of sediment transport pathways (Kraus 2000; Militello and Kraus 2001a). Here, we investigate sediment pathways at an idealized inlet with a coupled tide, wave, and sediment transport-morphology change numerical modeling system. The idealized inlet, ebb shoal, and channel were devised to test the coupled modeling system and identify sediment transport pathways driven by wave and tidal forcing (bypassing modes 1 and 2).

1) Coastal Analysis LLC, 4886 Herron Road, Eureka, CA 95503. CoastalAnalysis@cox.net.
2) U.S. Army Engineer Research and Development Center, Coastal and Hydraulics Laboratory, 3909 Halls Ferry Rd., Vicksburg, MS 39180. Nicholas.C.Kraus@erdc.usace.army.mil.

Transport paths and morphology change were calculated for tide only, wave only, and combined tide and wave forcing by application of coupled circulation, wave, and sediment transport-morphology change models. Wave forcing was exaggerated by specification of a relatively large wave angle to induce strong morphologic response over short simulation intervals. This approach allows rapid testing to determine if calculated transport and morphologic change patterns are representative of those observed in nature.

The circulation model M2D (Militello and Zundel, 2003) has been coupled to the steady spectral wave model (STWAVE) (Smith et al. 2001) through the Surfacewater Modeling System (SMS). This coupling provides a method for representing multiple scales of motion, a situation prevalent in coastal dynamics owing to the presences of the tide, waves, and interaction of these processes including wave transformation and breaking (Militello et al. 2000). Radiation stress gradients from the wave model are mapped to the circulation model for calculation of the wave-induced current. Depth-integrated currents from the circulation model are mapped to the wave model for calculation of wave-current interaction. Sediment transport is calculated through the total sediment load formulation of Watanabe (1987) as one of several sediment-transport formula options. This coupled system calculates tidal propagation; the current driven by the tide, waves, and wind; sediment transport; and bottom morphology change.

COUPLED MODELS

Combined circulation and wave modeling was conducted with the Steering Module, a component of the SMS interface developed in the U.S. Army Corps of Engineers' Coastal Inlets Research Program that couples models at user-specified time steps called "steering intervals" (Zundel et al. 2000; Zundel et al. 2002). The Steering Module provides three options for coupling of M2D and STWAVE: (1) 1-way coupling STWAVE to M2D. Radiation stress gradients from STWAVE are input to M2D for wave-driven current calculations; (2) 1-way coupling of M2D to STWAVE. Current fields from M2D are input to STWAVE for calculation of wave-current interaction; and (3) 2-way coupling. Both 1-way coupling options are conducted to calculate wave-driven currents and wave-current interaction. For all simulations in this study that involved combined waves and tidal forcing, 2-way coupling was invoked. Coupling of the circulation and sediment transport models was achieved by implementing the Watanabe (1987) total-load formulation directly into M2D. Current velocity, ambient depth, water level, and bottom stress were input to the sediment transport model every 100 s. Sediment transport rates and updated values of depth over the model domain were calculated. The updated depths were then input to the circulation model so that the hydrodynamic responses to change in bathymetry were calculated. Sediment transport rates (median grain size of 0.2 mm) were output periodically, from which sediment-transport paths can be identified. Time-varying depths were also output to examine morphology change.

SIMULATION SPECIFICATIONS

An idealized grid was developed such that the inlet, channel, ebb shoal, and bay dimensions approximate those of Shinnecock Inlet. Ocean and inlet grid dimensions are 15 km alongshore, 5 km from the shoreline to the ocean boundary, and inlet length and width of 500 m and 300 m, respectively. Bay dimensions are 1.5 km × 5 km, with depth of 5 m, giving a total volume of 37.5 M m^3, approximating that of Shinnecock Bay. Inlet depth was specified as 5 m, and the minimum depth of the spherical ebb shoal was 2 m, similar to that at Shinnecock Inlet, and at the approximate same distance offshore (Fig. 1). (The idealized grid is rotated approximately 90 deg

clockwise from Shinnecock Inlet.) Dual parallel jetties extend 250 m seaward from the shoreline. Calculation cells were specified to be 25 m on each side for the wave model giving fine resolution for the breaking waves. Cell side lengths varied between 25 and 50 m for the circulation model, with finer resolution near the shore and through the inlet. The Manning roughness coefficient, specified in the circulation model, varied between 0.028 $m/s^{1/3}$ in the offshore region to 0.04 $m/s^{1/3}$ in the inlet and surf zone.

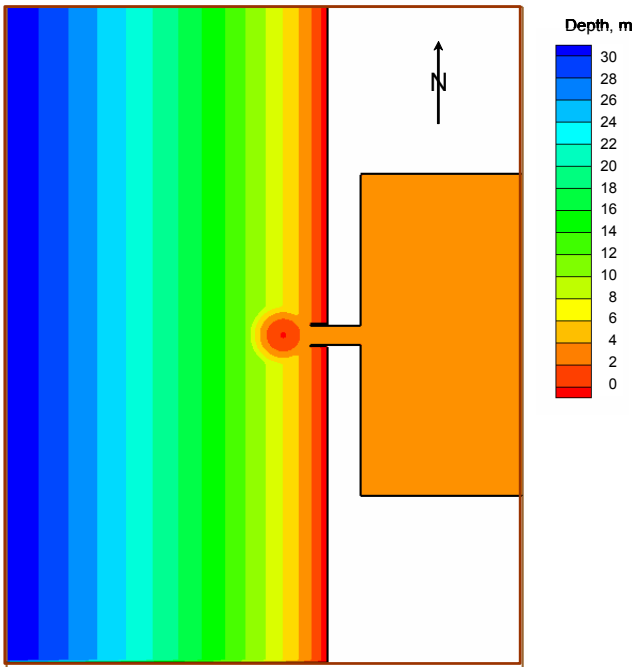

Fig. 1. Idealized grid bathymetry

Five simulations were conducted in which combinations of tide and wave forcing were applied (Table 1). For the case of tide forcing only, no coupling with the wave model was conducted. For the cases with wave forcing only, 1-way coupling was conducted in which radiation stress gradients were transferred from the wave model to the circulation model and were held constant throughout the simulation. For cases with both wave and tide forcing, 2-way coupling was invoked at 3-hr steering intervals.

Table 1. Simulation Properties

Case Number & Description	Tide Range, m	Wave Height*, m	Wave Period*, s	Wave Direction*, deg
1. Tide only	1.0	0.0	0	0
2. Fair-weather wave only	0.0	1.0	8	30
3. Storm wave only	0.0	3.0	10	30
4. Tide & fair-weather wave	1.0	1.0	8	30
5. Tide & storm wave	1.0	3.0	10	30

* Wave properties refer to the significant wave height and peak spectral period specified in 30 m of water at the seaward STWAVE boundary..

Tide forcing for the circulation model was represented as a sine wave having amplitude of 0.5 m and period of 12.42 hr. For simulations in which no tide forcing was applied, the water-surface elevation at the offshore boundary was set constant to 0 m. Wave height and period were representative of fair-weather and storm conditions, and a narrow spectrum was specified. A time step of 1 s was applied for all circulation model simulations and model forcing was spun up for duration of 1 day with a hyperbolic tangent ramp function. Simulation duration was 99 hr.

HYDRODYNAMIC PROPERTIES

Current and wave fields for the five simulations are presented. Results from simulations with tidal forcing are shown at peak flood (hr 75) and peak ebb (hr 81). Results from simulations with wave-forcing only show the current field at the end of the simulation (hr 99). Contour scales for the velocity plots vary for each case to best represent the range of speeds calculated.

Case 1: Tide Only

Current speed and direction at peak flood and peak ebb for forcing by tide alone are shown in Figs. 2 and 3, respectively. In these and following similar figures, the entire domain is shown in panel A on the left, and detail at the ebb shoal and inlet is shown in panel B on the right. During flood, the strongest currents, reaching 0.9 m/s are located directly adjacent to the jetty tips. Inside the inlet, the strongest current speed is 0.65 m/s. On ebb, the maximum current speed is 0.71 m/s and occurs inside the inlet. The ebb shoal deflects the ebb current, splitting the jet. Maximum current speed over the shallowest portion of the ebb shoal is 0.3 m/s.

Case 2: Fair-Weather Wave

Wave height and direction for the fair-weather wave case are shown in Fig. 4. Strong refraction, wave shoaling, and breaking occur at and near the ebb shoal. Wave height ranges from 1 m at the seaward boundary to 1.8 m on the northeast edge of the ebb shoal.

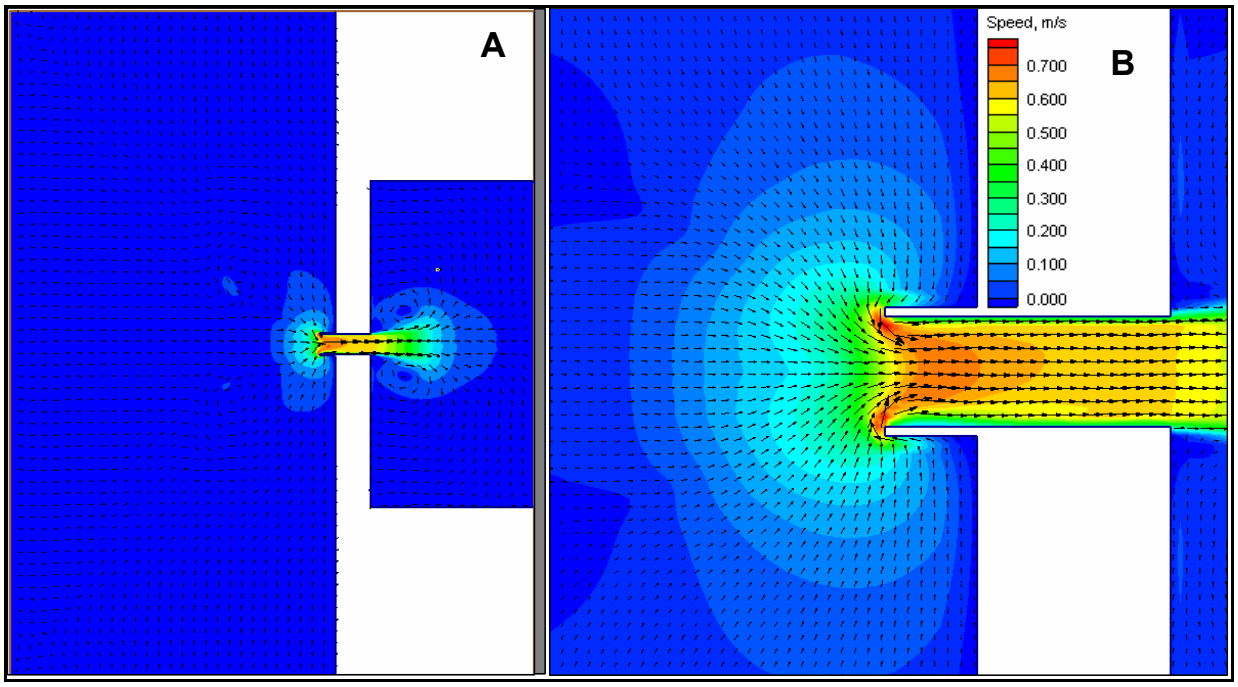

Fig. 2. Current speed and direction, peak flood (hr 75), tide only

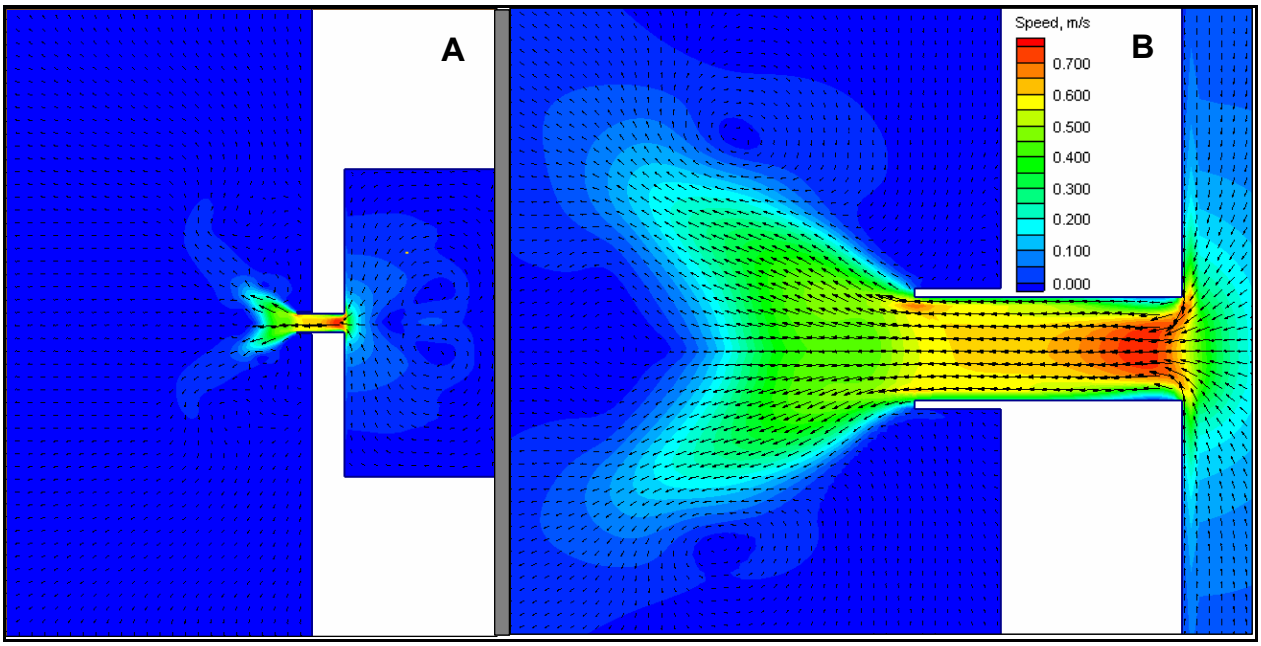

Fig. 3. Current speed and direction, peak ebb (hr 81), tide only

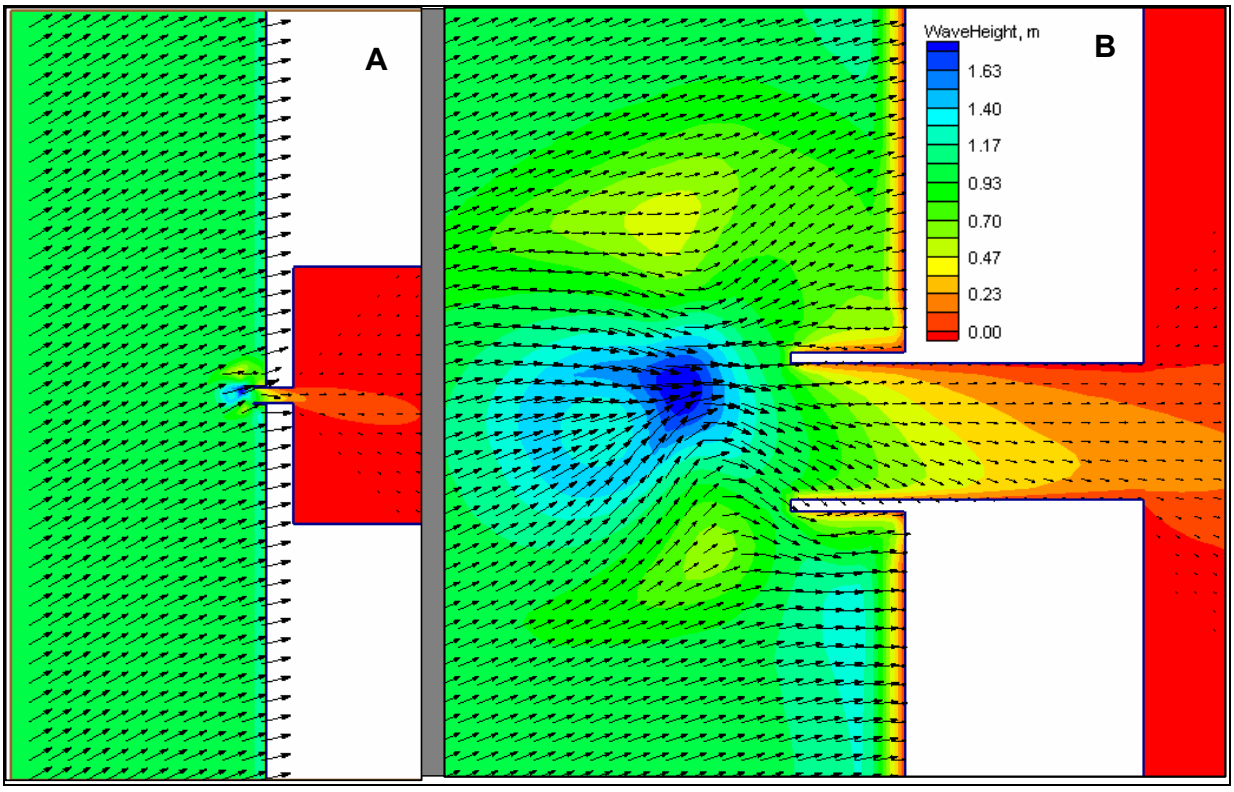

Fig. 4. Wave height and direction, fair-weather wave

Current speed and direction forced by the fair-weather wave is shown in Fig. 5. Wave shoaling, refraction, and breaking on the ebb shoal generate complex and strong currents there reaching 1.2 m/s. The surf zone is approximately 100 m wide and north-directed currents of 1.1 m/s are calculated there as a result of the wave forcing.

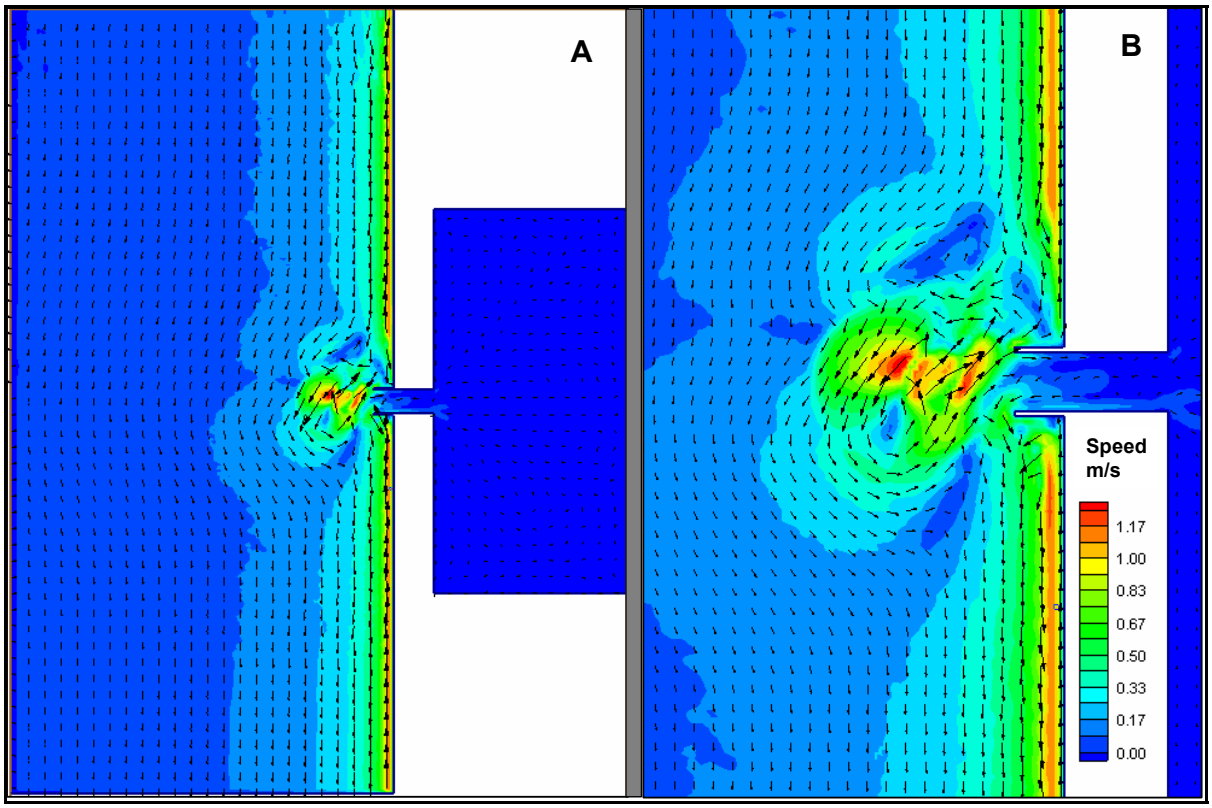

Fig. 5. Current speed and direction, fair-weather wave

Case 3: Storm Wave

Wave height and direction for the storm wave case are shown in Fig. 6. Strong refraction, wave shoaling, and breaking occur at and near the ebb shoal. Wave height ranges from 3 m at the seaward boundary to 3.5 m on the outer edge of the ebb shoal. Asymmetrical breaking takes place around the ebb shoal with waves breaking further seaward north of the shoal as compared to south of it.

Current speed and direction are shown in Fig. 7. The surf zone extends from the beach to approximately 250 m seaward, shifting the maximum longshore current speed away from the beach, as compared to the fair-weather wave case. Breaking waves on the ebb shoal produce strong northward flow over the central shoal area, and southward flow around the outer perimeter. In addition, a rip current forms off of the south jetty.

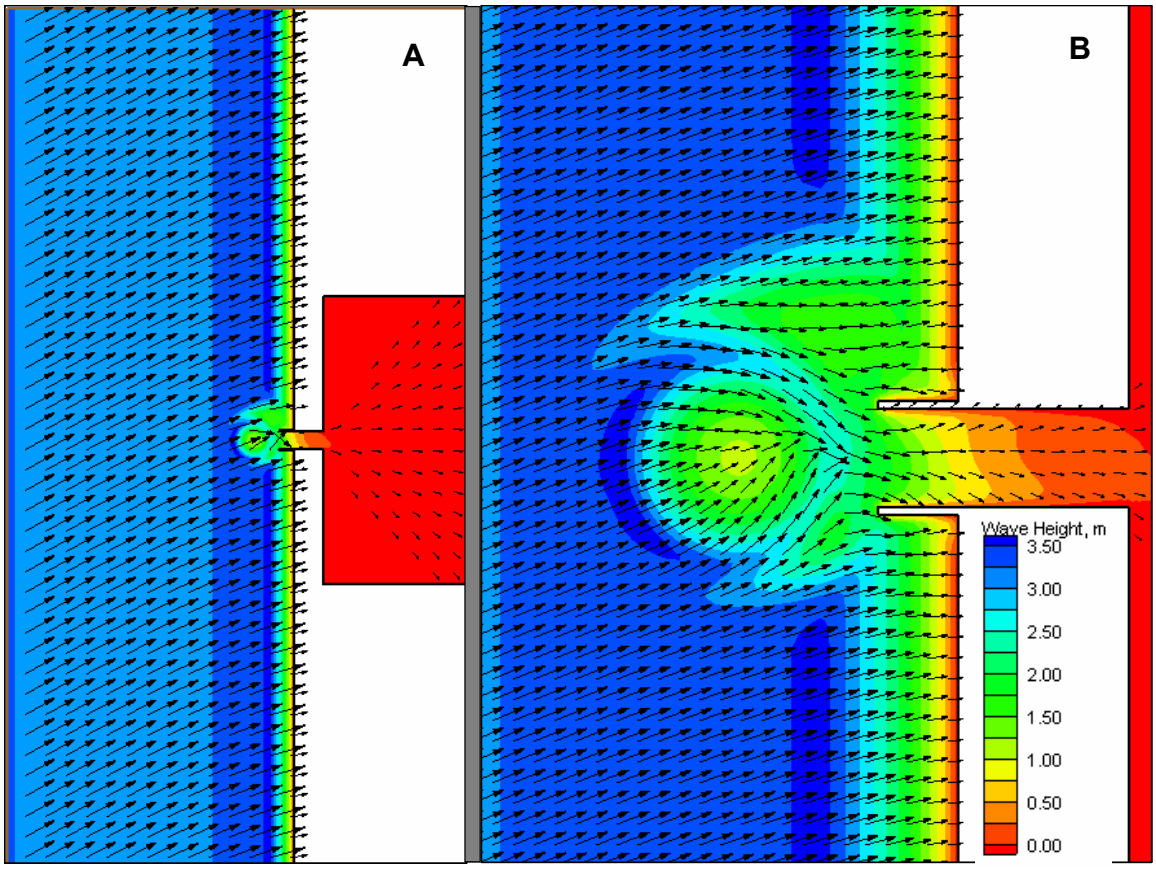

Fig. 6. Wave height and direction, storm wave

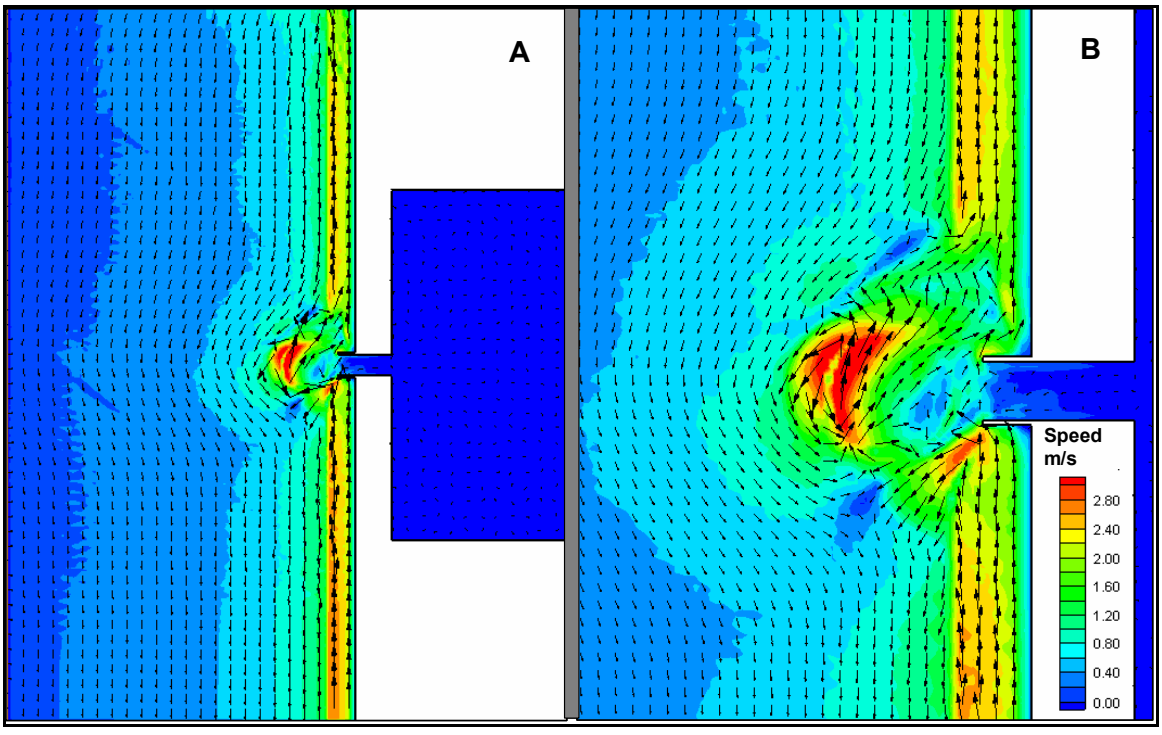

Fig. 7. Current speed and direction at hr 99, storm wave only

Case 4: Tide and Fair-Weather Wave

Current speed and direction forced by the tide and fair-weather wave are shown in Fig. 8 for flood and ebb. On the ebb shoal and in the surf zone, the current pattern and speed are similar to the fair-weather wave-only case. Currents in the inlet exhibit the properties of the tide, including strong speed at the jetty tips on flood.

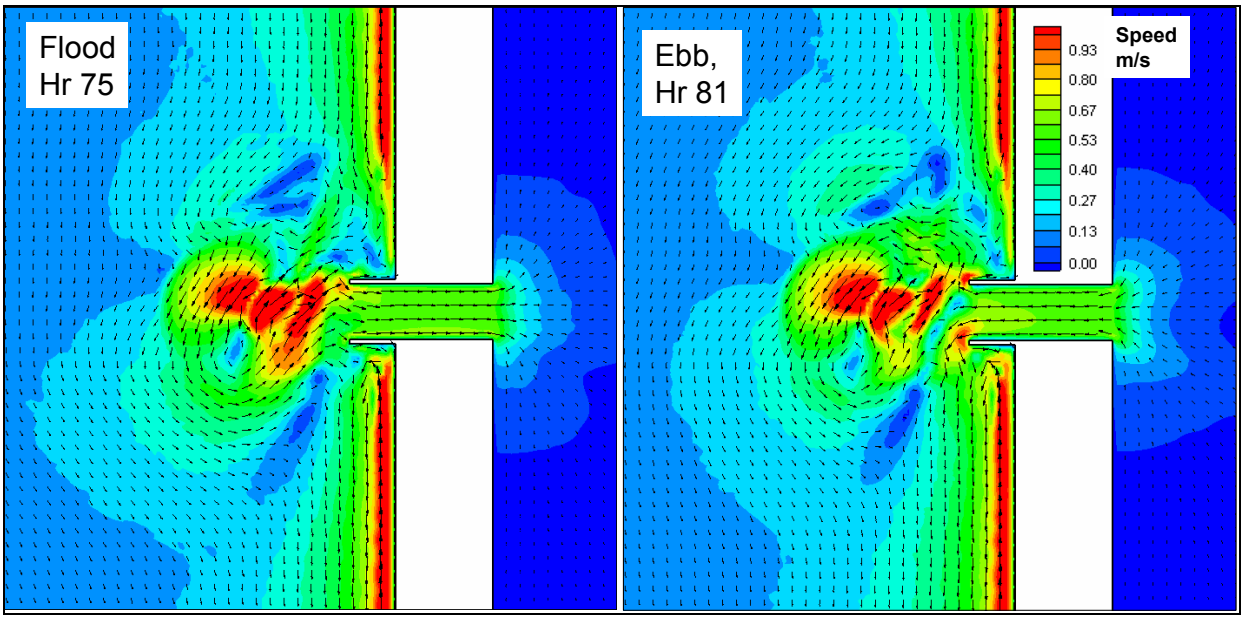

Fig. 8. Current speed and direction at peak flood (hr 75) and peak ebb (hr 81), tide and fair-weather wave

Case 5: Tide and Storm Wave

Current speed and direction for the situation of tide and storm waves are shown in Fig. 9 for flood and ebb. Current strength and pattern closely follow that of the storm-only currents, indicating the dominance of the waves. The inlet does exhibit tidal flow that increases the speed inside the inlet and between the jetty tips on both flood and ebb, as compared to the wave only case.

SEDIMENT PATHWAYS AND MORPHOLOGY CHANGE

Sediment transport rate vectors and morphology change are discussed for the five simulations. Contours show change in depth, with blue denoting increased depth (erosion) and yellow/red denoting decreased depth (accretion). Contour scales vary between the plots.

Case 1: Tide Only

Change in depth and transport vectors for the tide-only simulation are shown in Fig. 10 during flood and ebb. Maximum change takes place at the jetty tips where 0.5 m of erosion occurs. Erosion also takes place at the inlet entrances on both ocean and bay sides. Tip shoals form near the seaward end of the jetties. These changes in morphology replicate those that occur in nature and indicate that the sediment transport component of the modeling is realistic. No significant sediment bypassing occurs across the ebb shoal, and sediment enters the channel from both sides during flood tide, from where it can move to the ebb shoal and flood shoal.

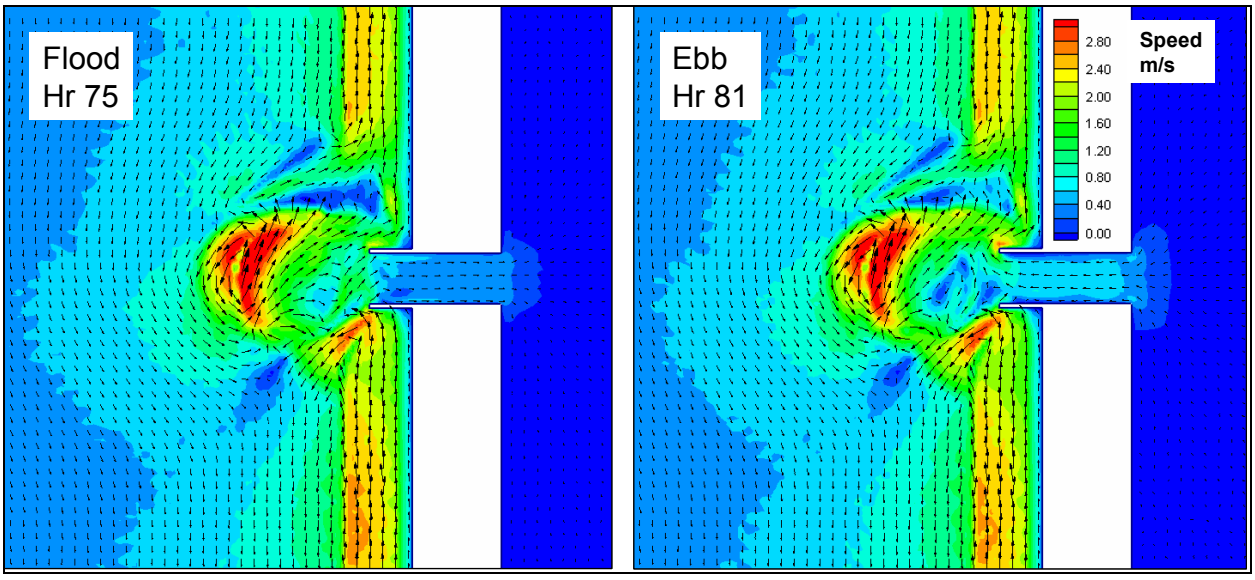

Fig. 9. Current speed and direction, peak flood (hr 75) & peak ebb (hr 81), tide & storm wave

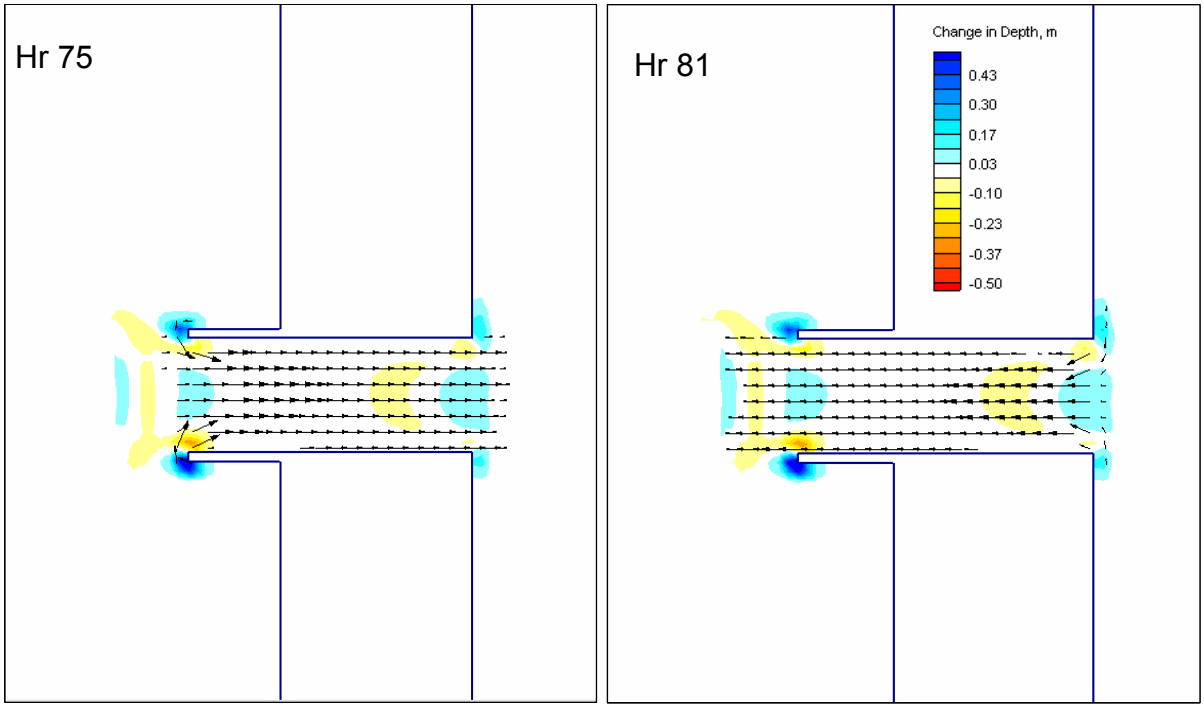

Fig. 10. Change in depth and transport vectors at hrs 75 and 81, tide only

Case 2: Fair-Weather Wave

Transport vectors and change in depth at hr 99 of the fair-weather wave simulation are shown in Fig. 11. Sand is impounded against the south jetty, as expected. North of the north jetty, erosion adjacent to the beach takes place. These morphologic changes indicate successful representation of morphology change at a beach near a jettied shoreline. Sediment is removed from the inner portion of the ebb shoal and bypassed. There is also some rearrangement of

material on the ebb shoal (moving the idealized shoal shape toward equilibrium). Material also enters the channel, moving around the updrift jetty, and would contribute to tidal bypassing.

The ebb shoal deepens in its central area and shallows on its seaward and northeast flanks. Transport vectors on the shoal indicate that material bypasses from the central shoal area to the regions of deposition. Morphology change on the shoal indicates an overall spreading pattern taking place, as the bathymetry moves toward an equilibrium state with the hydrodynamics.

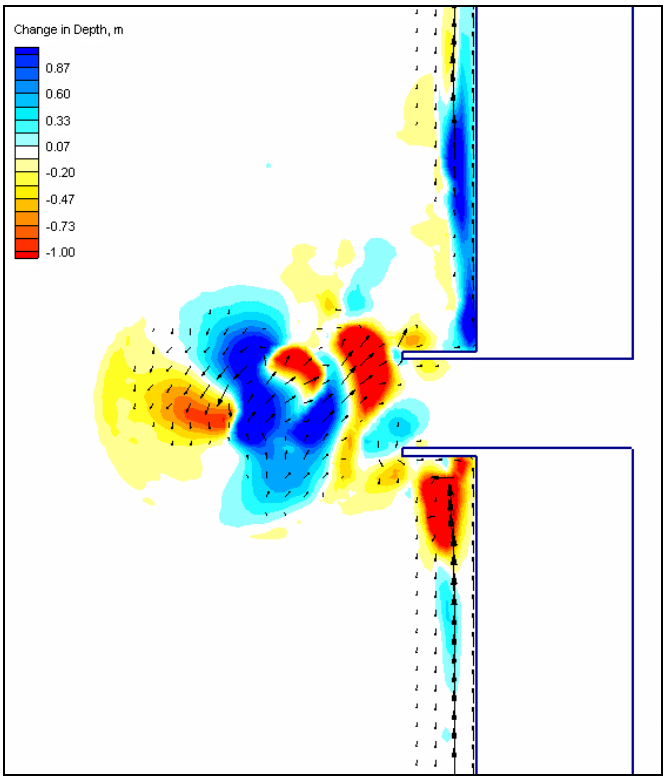

Fig. 11. Change in depth and transport vectors at hr 99, fair-weather wave

Case 3: Storm Wave

Morphology change and transport vectors at hr 99 from the storm wave simulation are shown in Fig. 12. Little accretion occurs at the south jetty because the surf zone current forms a rip at the jetty. Sand then deposits in a deltaic form located southeast of the ebb shoal. Erosion along the beach north of the north jetty also takes place. Scour holes form at the intersection where the north jetty meets the beach and in an area centered approximately 500 m north of the jetty (the jetty is 250 m long). Breaking waves on the ebb shoal transport material to the north and west, spreading the shoal over a wider area. Material is also transported and deposited inside the south jetty as a tip shoal. Morphology change on the ebb shoal for the storm waves has a different pattern than for fair- weather waves, with deposition taking place around most of the perimeter of the shoal. The fair-weather waves produce a splitting pattern in transport where deposition takes place on different sides of the shoal. The storm wave produces shoaling in the inlet near the south jetty and erosion at the north jetty. The fair-weather wave produces erosion at the south jetty, and a mixed erosion and accretion pattern at the north jetty. These differences at the inlet entrance and the ebb shoal owe to the different patterns of wave refraction, shoaling, and breaking on the shoal for the storm and fair-weather waves. Bypassing bars also form up-and

down drift of the ebb shoal. Bypassing occurs by sediment entering the channel from the south (updrift), and it can then be moved offshore by tide, as well as by material transported from the ebb shoal.

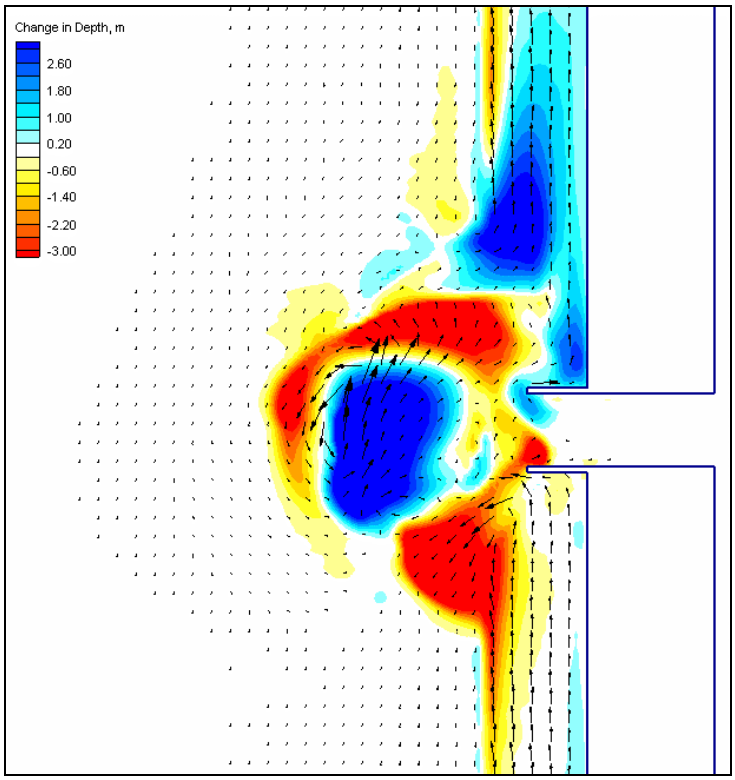

Fig. 12. Change in depth and transport vectors at hr 99, storm wave

Case 4: Tide and Fair-Weather Wave

Morphology change and transport vectors for combined tide and fair-weather wave forcing are shown in Fig. 13 at flood and ebb. Patterns of morphology change are similar to those for the fair-weather wave simulation (no tide) (Fig. 11), indicating that the waves are the dominant transport mechanism. However, the tidal currents do modify the transport patterns. The tip of the north jetty experiences greater erosion with tide and waves than with waves only, and the tip of the south jetty experiences less erosion. Comparison of Figs. 10, 11, and 13 indicates that waves dominate the bypassing and move material over the ebb shoal. In the interior of the inlet, transport by tide dominates that of waves.

Case 5: Tide and Storm Wave

Transport vectors and morphology change for the tide combined with storm waves are shown in Fig. 14. Changes in bathymetry for this simulation show little difference from the case with storm waves only, indicating the dominance of the waves in sediment transport. The most notable difference between the two simulations (Figs. 12, 14) is that the distance material is transported northward from the ebb shoal is reduced with the presence of the tide (the red band on the north side of the shoal is wider in the case with tide only). A reduction in the material carried away from the shoal in this region probably owes to flood tidal currents that weaken the north-directed wave-driven currents over the northern portion of the ebb shoal.

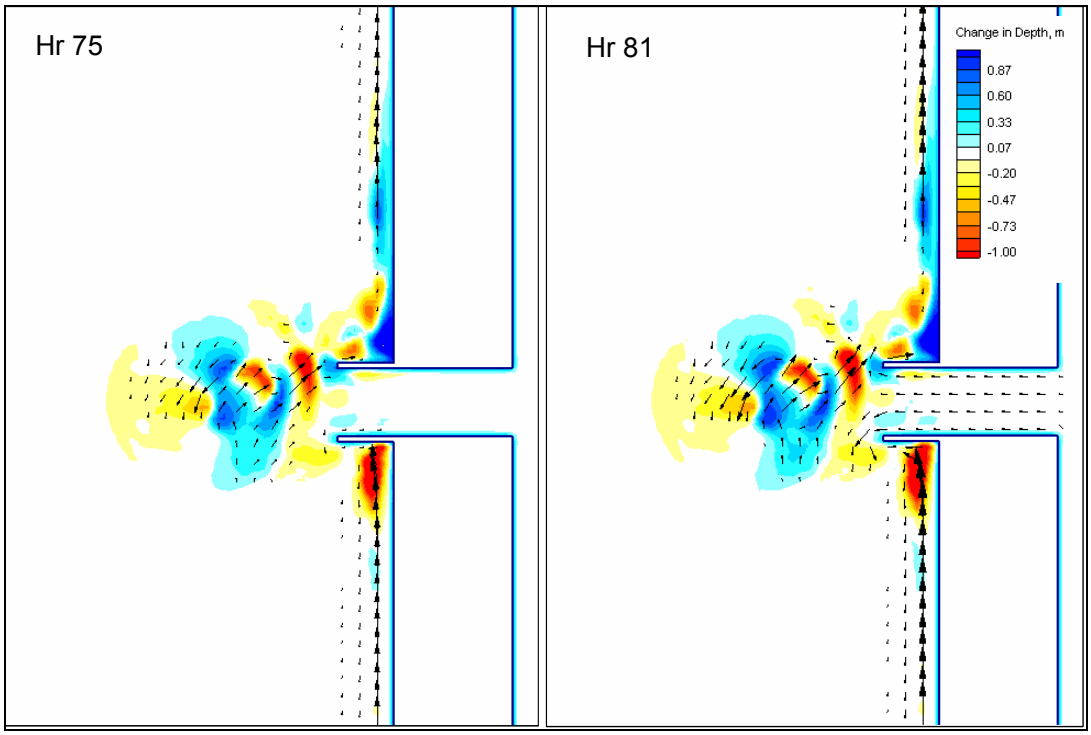

Fig. 13. Change in depth and transport vectors at peak flood (hr 75) and peak ebb (hr 81), tide and fair-weather wave

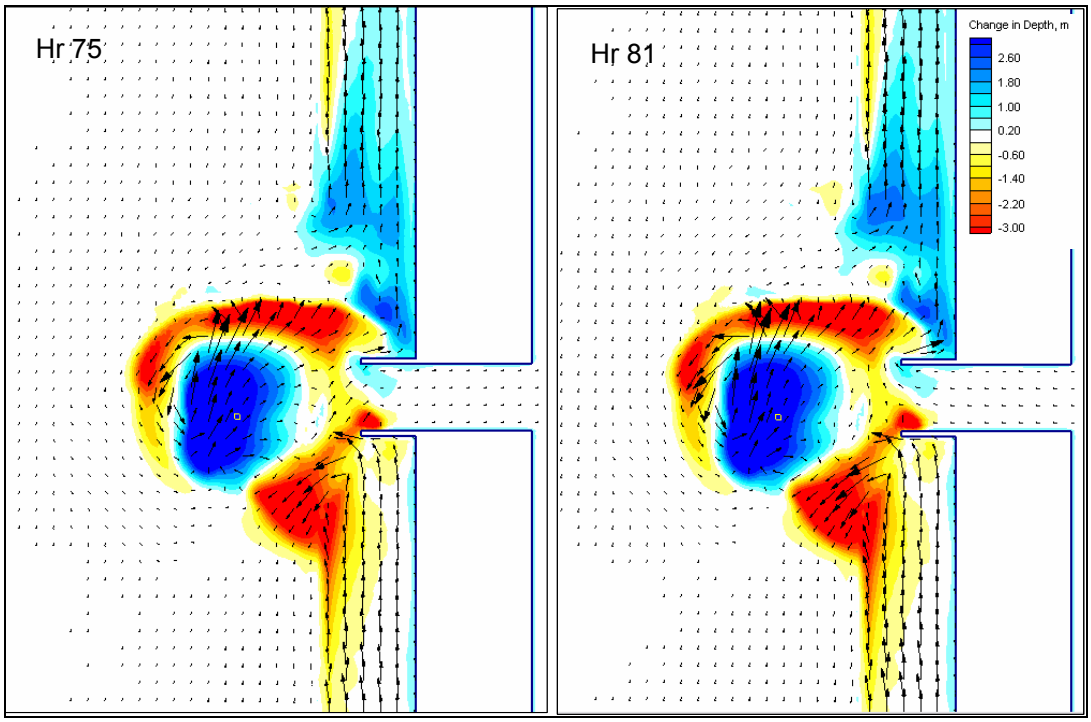

Fig. 14. Change in depth and transport vectors at peak flood (hr 75) and peak ebb (hr 81), tide and storm wave

CONCLUSIONS

A coupled wave, circulation, and sediment transport modeling system was applied to an idealized inlet and ebb shoal to examine the physical response to tide and wave forcing. The idealized inlet was patterned after Shinnecock Inlet, New York, in dimensions, geometry, jetty configuration, bay area, and morphology. Five simulations were conducted for combinations of tide, fair-weather waves, and storm waves. Wave direction was specified at 30 deg to produce exaggerated and rapid response from the modeling system to allow multiple simulations over brief time intervals. Changes in depth from wave forcing were greater than would be expected over the same duration at a real inlet.

Patterns of response of the current to tide and waves reproduced those that are commonly observed to occur at tidal inlets stabilized by jetties. Well-defined longshore currents developed nearshore. The longshore current speed increased with larger waves, and the surf zone and location of peak current moved further offshore. Wave refraction and breaking on the ebb shoal produced strong and complex currents. For both fair-weather and storm waves, a strong north directed flow was produced on the central and northern portion of the ebb shoal, while a south-directed current formed on the outer shoal.

Calculation of morphology change showed realistic patterns for both wave and tidal forcing. Erosion at the jetty tips took place under tidal flow, as well as formation of tip shoals. Sand transport by waves impounded material against the south jetty during fair-weather conditions. During storm conditions, sand from the updrift nearshore region was moved to a deltaic formation off the tip off the south jetty. Both storm and fair-weather waves eroded the top of the ebb shoal and deposited material along its north and western perimeter. Fair-weather waves produced a split deposition pattern on the ebb shoal perimeter, whereas storm waves produced a spatially continuous band of deposition. These patterns resulted in a skewed ebb shoal. Storm waves produced scour at the tip of the downdrift jetty, in part controlled by phasing of the tide alongshore.

Updrift and downdrift bypassing bars formed under wave action. The modeling results thus give support to the Reservoir Model (Kraus 2000) concept of ebb shoal morphology genesis, in which the ebb shoal proper is developed by transport from the ebb jet, and the bypassing bars and lobes of the ebb shoal are created by transport under wave action.

ACKNOWLEGEMENTS

This paper was prepared under the Inlet Modeling System Work Unit of the Coastal Inlets Research Program, U.S. Army Corps of Engineers. Permission was granted by Headquarters, U.S. Army Corps of Engineers, to publish this information.

REFERENCES

Bruun, P., and Gerritsen, F. 1959. Natural By-Passing of Sand at Coastal Inlets. *J. of Waterways and Harbors Division*, ASCE, WW4, 75-107.

Gaudiano, D. J., and Kana, T. W. 2000. Shoal Bypassing in South Carolina Tidal Inlets: Geomorphic variables and empirical predictions for nine mesoscale inlets," *Journal of Coastal Research* 17(2), 280-291.

Kraus, N. C. 2000. Reservoir Model of Ebb-Tidal Shoal Evolution and Sand Bypassing. *Journal of Waterway, Port, Coastal, and Ocean Engineering*, 126(3), 305-313.

Militello, A., and Kraus, N. C. 2000. Regional Coastal and Inlet Circulation Modeling with Application to Long Island, New York. *Proc of the 2000 National Conference on Beach Preservation Technology*, Florida Shore & Beach Preservation Association, Tallahassee, Florida, 191-201.

Militello, A., and Kraus, N. C. 2001a. Shinnecock Inlet, New York, Site Investigation Report 4, Evaluation of Flood and Ebb Shoal Sediment Source Alternatives for the West of Shinnecock Interim Project, New York. Coastal Inlets Research Program, Tech. Rpt. CHL-98-32, U.S. Army Engineer Research and Development Center, Vicksburg, MS.

Militello, A., and Kraus, N. C. 2001b. Re-alignment of an Inlet Entrance Channel by Ebb-Tidal Eddies. *Proc of the Coastal Dynamics 2001 Conference*, ASCE, 423-432.

Militello, A., Kraus, N. C., Rahoy, D. S., Couch, S., and Weppler, P. M. 2001. Establishment of a Flood Shoal Sand Source with Preservation of Existing Habitat Function. *Proc of the 2001 National Conference on Beach Preservation Technology*, Florida Shore & Beach Preservation Association, Tallahassee, FL, 327-341.

Militello, A., and Zundel, A. K. (2003) Two-Dimensional Circulation Model M2D: Report 1, Technical Documentation and User's Guide. Coastal Inlets Research Program, Tech. Rpt. ERDC-CHL-TR-___, U.S. Army Engineer Research and Development Center, Vicksburg, MS (in press).

Smith, J. M., Sherlock, A. R., and Resio, D. T. 2001. STWAVE: Steady-State Spectral Wave Model: User's Manual for STWAVE Version 3.0. Supp. Rpt. ERDC/CHL SR-01-1, U.S. Army Engineer Research and Development Center, Vicksburg, MS.

Watanabe, A. 1987. 3-dimensional Numerical Model of Beach Evolution. *Proc Coastal Sediments '87*, ASCE, 802-817.

Zundel, A. K., Militello, A., Cialone, M., and Moreland, T. 2002. SMS Steering Module: An Interface for Automated Coupling of Circulation and Wave Models. *Seventh International Estuarine and Coastal Modeling Conference*, ASCE Press, New York, 310-328.

Zundel, A. K., Militello, A., and Gonzales, D. S. 2000. Numerical Model Steering Module – Let the Communication Begin. *Proc. 4th International Conference on Hydroinformatics*, International Association of Hydraulic Research, Cedar Rapids, Iowa, Abstract Volume p. 206, CD-ROM -IT-3:227-1099.pdf.

Keywords: Tidal inlet, sediment bypassing, numerical modeling, morphology change, Shinnecock Inlet, New York